Construction and Building Materials 366 (2023) 130187

Contents lists available at ScienceDirect

Construction and Building Materials

journal homepage: www.elsevier.com/locate/conbuildmat

Comparative study of indirect tensile test and uniaxial compression test on asphalt mixtures: Dynamic modulus and stress-strain state

Hao Chen [a,*], Mequanent Mulugeta Alamnie [b], Diego Maria Barbieri [a,c], Xuemei Zhang [a], Gang Liu [d], Inge Hoff [a]

[a] Department of Civil and Environmental Engineering, Norwegian University of Science and Technology, Trondheim 7491, Norway
[b] Department of Engineering Sciences, University of Agder, Grimstad 4879, Norway
[c] Department of Mechanical and Structural Engineering and Materials Science, University of Stavanger, Stavanger 4021, Norway
[d] School of Materials Science and Engineering, Wuhan University of Technology, Wuhan 430070, China

ARTICLE INFO

Keywords:
Indirect tensile test
Uniaxial compression test
Asphalt mixture
Master curve
Dynamic modulus
Stress–strain state

ABSTRACT

Dynamic modulus is an essential parameter for the performance characterisation of asphalt materials for performance prediction and pavement design. The Indirect Tensile (IDT) test and the Uniaxial Compression (UC) test are both well-known experiments performed in the laboratory to characterise the dynamic modulus of asphalt mixtures over a range of temperatures and loading frequencies. A considerable amount of research has investigated the difference between two test modes, while few studies analysed the fundamental difference in stress–strain distributions for the two test setups. This work aims at comparing the effect of the two test methods on dynamic modulus of asphalt mixtures, as well as stress–strain state. For these purposes, two types of mixtures commonly employed to build road surface layers, namely Asphalt Concrete (AC) and Stone Mastic Asphalt (SMA), were created and tested. The specimens were prepared with a gyratory compactor. The master curves of dynamic modulus and the stress–strain states obtained from the two testing procedures were compared. The dynamic modulus and phase angle results are almost identical for medium frequency and temperature, whereas the results exhibit significant discrepancies for lower and higher frequency values. AC 11 and SMA 11 mixtures show differences in comparison between the two tests. Moreover, the strains measured by the IDT test are variable and the strains obtained from the UC test stabilise around 40 με. Similarly, both tests have poor strain control at 40 °C. The values of normalised stresses measured by the IDT test are approximately 3.26 and 2.34 times greater than the ones measured by the UC test for AC 11 and SMA 11 mixtures, respectively. In general, the results of the mechanical characterisation of the asphalt mixtures conducted using both tests are similar. The IDT test has the advantage of sample size for sample preparation methods in both laboratory and field, and the UC test has a better deformation control at low and medium temperatures.

1. Introduction

In the development of pavement design, the Mechanistic-Empirical (ME) pavement design approach applicable to various materials and environmental conditions has been gradually adopted to replace previous empirical design approaches [1,2]. The mechanical characterisation of road construction materials is necessary to predict the response of the structure according to the ME pavement design. When it comes to asphalt materials, the dynamic modulus is an essential parameter for engineering computations [3]. The dynamic modulus of asphalt mixtures mainly depends on the temperature and the loading time due to its viscoelastic properties [4–6]. The Uniaxial Compression (UC) test, which can be conducted at different temperatures and frequencies with a dynamic loading form, is the standard test method for the determination of dynamic modulus of asphalt mixture in the ME pavement design guide [7]. The dynamic modulus is calculated by dividing the peak-to-peak stress by the peak-to-peak strain for the asphalt mixture subjected to a sinusoidal load. Afterwards, the dynamic modulus master curve is constructed according to the time–temperature superposition principle [8] to predict the dynamic modulus of asphalt mixture over a

* Corresponding author.
E-mail addresses: hao.chen@ntnu.no (H. Chen), mequanent.m.alamnie@uia.no (M.M. Alamnie), diegomb271@gmail.com (D.M. Barbieri), xuemei.zhang@ntnu.no (X. Zhang), liug@whut.edu.cn (G. Liu), inge.hoff@ntnu.no (I. Hoff).

https://doi.org/10.1016/j.conbuildmat.2022.130187
Received 10 October 2022; Received in revised form 25 November 2022; Accepted 20 December 2022
Available online 26 December 2022
0950-0618/© 2022 The Author(s). Published by Elsevier Ltd. This is an open access article under the CC BY license (http://creativecommons.org/licenses/by/4.0/).

Table 1
Physical properties of bitumen 70/100.

Physical property	Unit	Bitumen 70/100	Test standard
Penetration at 25 °C	0.1 mm	92	EN 1426:2015 [22]
Softening point (Ring and Ball)	°C	46.0	EN 1427:2015 [23]

Table 2
Resistance to wear and fragmentation of crushed rock aggregates.

Property	Value	Requirements for AADT > 15 000	Test standard
Micro-Deval coefficient	14.2	≤ 20	EN 1097–1:2011 [24]
Los Angeles value	18.2	≤ 15	EN 1097–2:2020 [25]

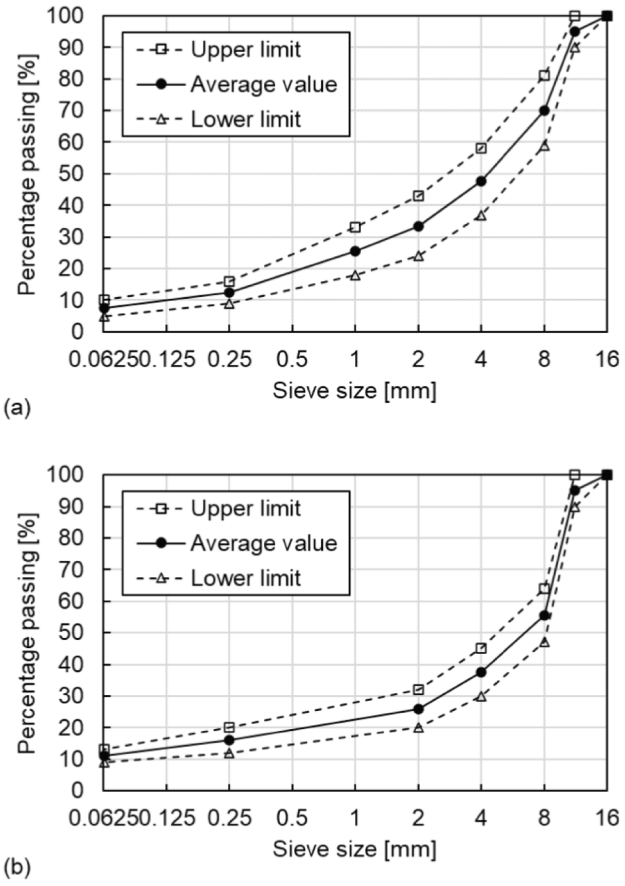

Fig. 1. Grading curves of (a) AC 11 and (b) SMA 11.

Table 3
OBC and voids characteristics of AC 11 and SMA 11.

Asphalt mixture	*OBC* [%]	Void characteristic (EN 12697–8:2018 [29])			
		V_a [%]	Standard deviation	*VFB* [%]	Standard deviation
AC 11	5.1 %	3.8 %	0.2 %	77.0 %	1.3 %
SMA 11	5.3 %	4.0 %	0.3 %	77.1 %	1.6 %

wide frequency range. This test method is widely used not only for traditional materials but also for innovative and recycled construction resources [9–11].

The dynamic modulus can be tested on samples produced in the laboratory or from samples cored from a real pavement. However, the thickness of the core sample extracted from the existing pavement is often less than the required height of the UC test. Differently, the Indirect Tensile (IDT) test determines the dynamic modulus according to a biaxial stress state on a thinner specimen [12]. Compared with UC test, the IDT test is largely used thanks to the easiness of operation (e.g., smaller samples) and its suitability to characterise core road samples. Even though the IDT test is commonly used for the evaluation of resilient modulus, strength and fatigue of asphalt mixture, it has been also performed to assess the dynamic modulus. Zaumanis et al. [13] conducted IDT investigation to determine the dynamic modulus of 100 % recycled asphalt mixtures while appraising the suitability of the IDT setup to characterise highly recycled asphalt mixtures. Mollenhauer et al. [14] obtained the stiffness of asphalt mixtures by conducting IDT tests to develop a German ME pavement design. Zhang et al. [15] have adopted the IDT test to compare the change in dynamic modulus of asphalt mixture before and after chemical ageing. The Norwegian Public Roads Administration (NPRA) is currently developing a ME pavement design system and, therefore, needs the creation of a database defining the dynamic modulus for the asphalt mixtures employed in the Nordics pavements [16].

Although both IDT and UC tests can measure the dynamic modulus of asphalt materials, their results show some discrepancies due to the different stress–strain states and test conditions [17]. Understanding these differences is important to select the correct material characterisation testing and to define the pavement design system more accurately. Kim et al. [18] developed an analytical solution to assess the dynamic modulus from the IDT test. In this regard, twelve asphalt mixtures used in North Carolina were tested according to both IDT and UC procedures. The results displayed a little discrepancy in the dynamic modulus master curves. However, Qin et al. [19] found some differences between the two tests in dynamic modulus, phase angle, and shift factor. The dynamic modulus and shift factor measured using the UC test were higher than the corresponding values obtained using the IDT test. As very few studies shed light on the differences between the IDT and the UC testing procedures from the perspective of stress–strain states for Norwegian asphalt mixtures, this work addresses this gap as well as delves into the fundamental difference in stress–strain distributions for the two test setups and provides guidance on test methods for the development of Norwegian ME pavement design.

In this study, Asphalt Concrete (AC) and Stone Mastic Asphalt (SMA) mixtures were characterised as they were commonly used for surfacing road pavements. The mixtures were compressed using a gyratory compactor and the samples were drilled and cut according to the testing requirements. The IDT and UC tests were conducted in the laboratories of the Norwegian University of Science and Technology (NTNU) and the University of Agder (UiA), respectively. The master curves were constructed based on the ME pavement design guide and shift factor function defined by the Williams-Landel-Ferry (WLF) equation. The differences in the values of dynamic modulus, phase angle, shift factor as well as the discrepancies in the stress–strain states for the two tests were analysed.

2. Materials and test methods

2.1. Materials

The bituminous binder employed was type 70/100, which is the most used in Norwegian asphalt pavements. Crushed rocks having magmatic and metamorphic origin as well as limestone filler were used as aggregates [20,21]. The main physical properties of the binder are given in Table 1. The resistance of aggregates to wear and fragmentation is

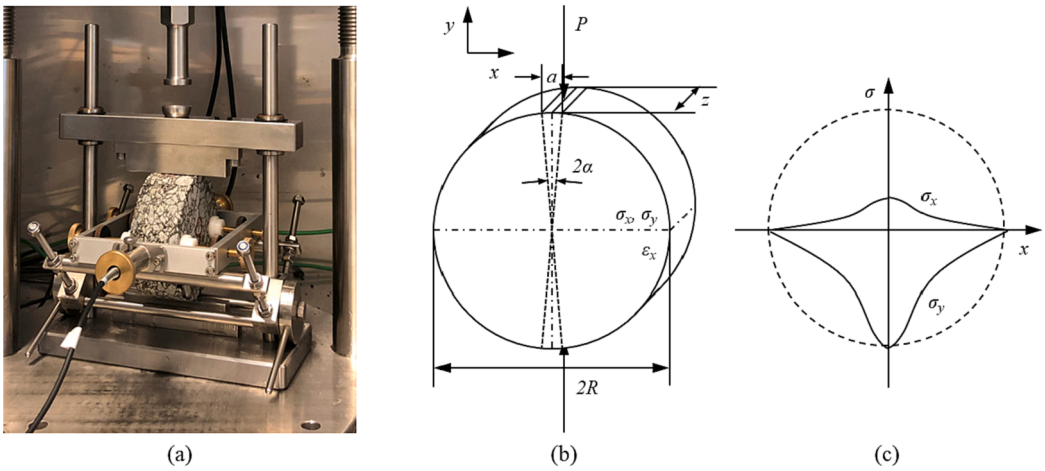

Fig. 2. (a) IDT test setup using UTM, (b) scheme of IDT test specimen subjected to a vertical load and (c) stress distribution.

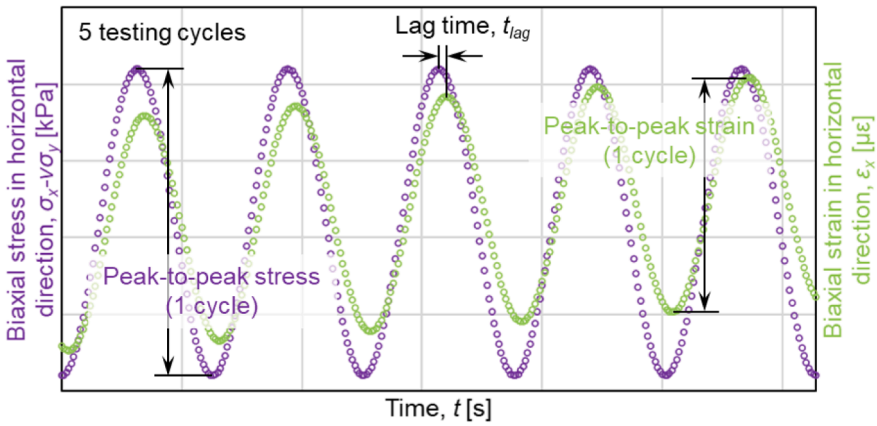

Fig. 3. Schematic trend of stress and strain for IDT test.

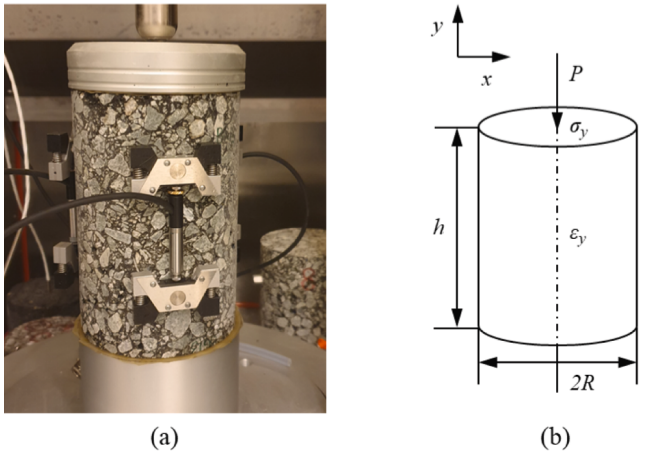

Fig. 4. (a) UC test setup using UTM-130 and (b) scheme of UC specimen subjected to a vertical load.

specified in Table 2, which fulfils the Norwegian requirements of AC and SMA mixtures with an Annual Average Daily Traffic (AADT) higher than 15 000.

2.2. Sample preparation

Sample preparation is very important for the results from laboratory testing of asphalt and special care was taken to produce samples as homogeneous as possible to compare the two testing methods without any bias from the sample preparation.

The particle size distributions are given in Fig. 1 and the average gradation curves are selected to prepare the tested samples. The Optimum Binder Content (*OBC*) was determined by the Marshall mixture design. The asphalt mixture specimens were prepared in the laboratory of NTNU using a gyratory compactor (ICT-150RB produced by Invelop Oy, Savonlinna, Finland). The compaction pressure was 620 kPa, and the gyratory angle was set to 17 mrad (0.97°) [26]. The 100 and 115 design gyrations were applied for the AC 11 and SMA 11, respectively [27]. Asphalt cylinders with a diameter of 150 mm and a height of 180 mm were thus obtained; afterwards, IDT specimens (diameter = 100 mm, height = 40 mm) and UC specimens (diameter = 100 mm, height = 150 mm) were drilled and cut. The *OBC* and the void characteristics including the Air Voids Content (V_a) and the Voids Filled with Binder (*VFB*) are shown in Table 3, which fulfil the corresponding requirements [28]. Four replicate samples were created for each asphalt mixture type.

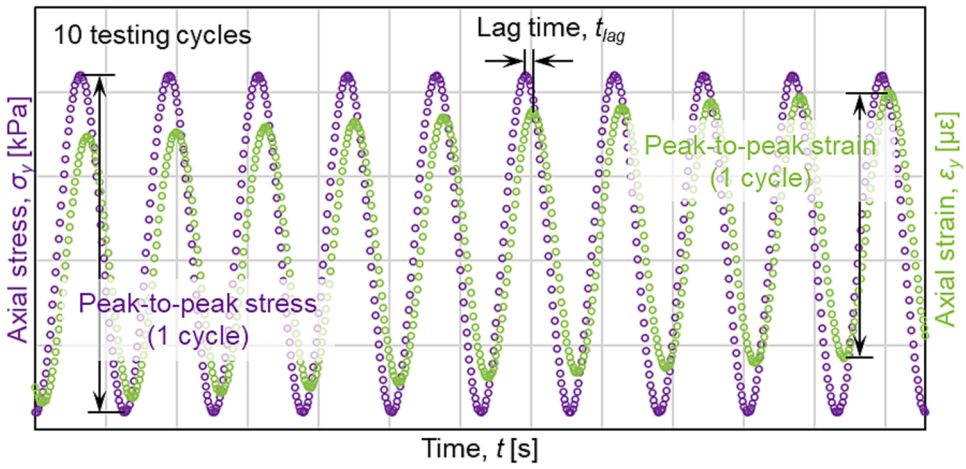

Fig. 5. Schematic trend of stress and strain for UC test.

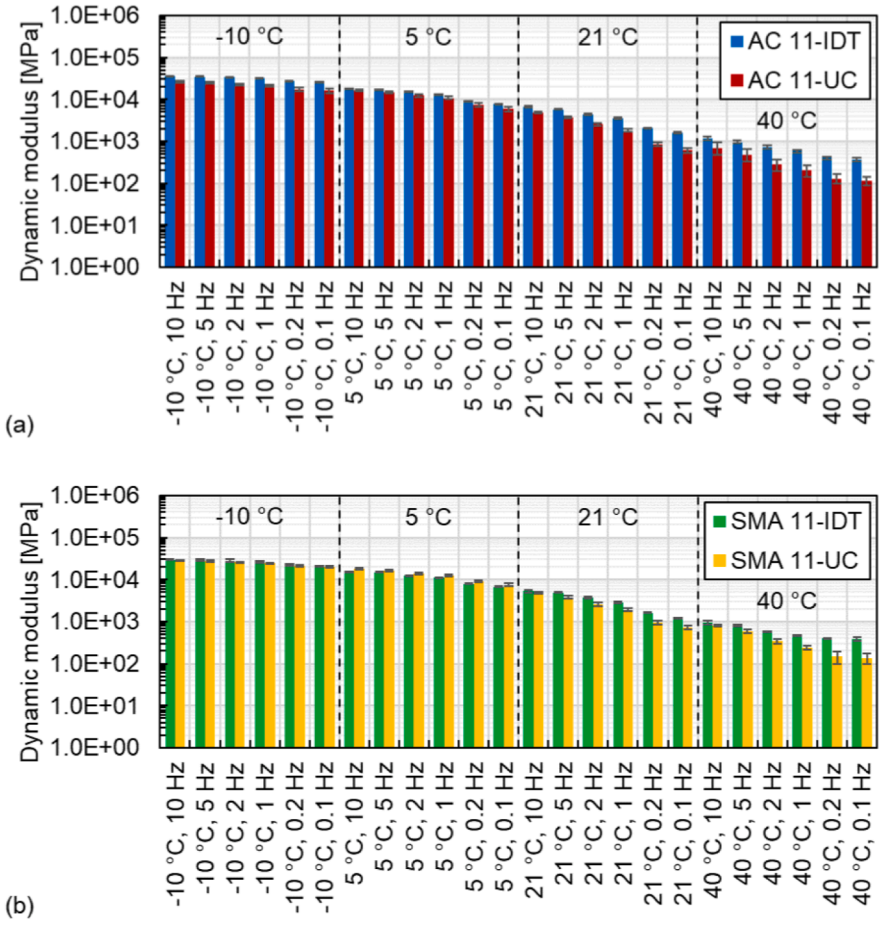

Fig. 6. Dynamic modulus results: (a) AC 11 and (b) SMA 11.

A total of 16 samples were tested and they were denominated as AC 11-IDT, AC 11-UC, SMA 11-IDT and SMA 11-UC.

2.3. Dynamic modulus tests

2.3.1. Indirect tensile test

The cyclic IDT test was performed by a servo-pneumatic Universal Testing Machine (UTM) produced by Cooper Technology exerting a controlled harmonic sinusoidal load with a haversine wave. Two Linear Variable Differential Transformers (LVDT) were used on both sides in the horizontal direction. The test was conducted in accordance with EN 12697–26 [30] at frequencies of 10, 5, 2, 1, 0.2 and 0.1 Hz and the temperatures of −10, 5, 21 and 40 °C to obtain a broad and continuous dynamic modulus master curve for measured values. The applied loads were adjusted to keep the initial horizontal strain amplitude in a range between 50 με to 100 με for every testing temperature and frequency. The IDT test is regarded as a stress–strain dual control test.

The scheme of the IDT test is shown in Fig. 2; the x and y axes are

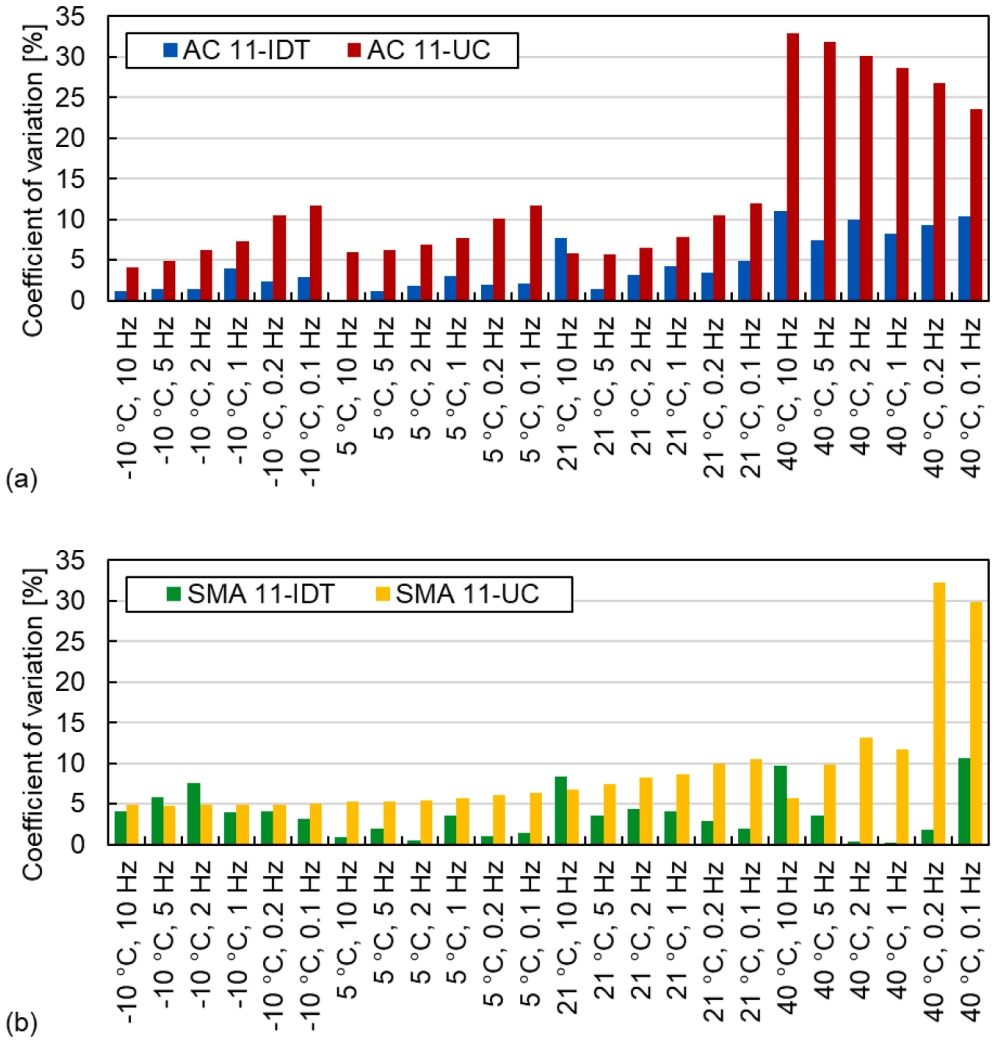

Fig. 7. Coefficient of variation of dynamic modulus results: (a) AC 11 and (b) SMA 11.

defined as the horizontal and vertical direction, respectively. Based on the linear viscoelastic solution the stress and strain in the horizontal direction of the IDT test specimen are used to calculate the dynamic modulus [18]. The stress distribution is presented in Fig. 2(c). The coordinate axis between the position in the horizontal direction and the stress at this position was established. The IDT test specimen was applied a vertical harmonic sinusoidal load, P, which can be expressed as shown in Eq. (1). Along the horizontal diameter of the IDT specimen the horizontal stress, $\sigma_x(x)$, and the vertical stress, $\sigma_y(x)$, can be evaluated as defined by Eq. (2) and Eq. (3), respectively [31–33].

$$P = P_0 \cdot e^{i\omega t} = P_0[\cos(\omega t) + i\sin(\omega t)] \tag{1}$$

$$\sigma_x(x) = \frac{2P}{\pi a z}\left[\frac{(1-x^2/R^2)\sin 2\alpha}{1+2(x^2/R^2)\cos 2\alpha + x^4/R^4} - \tan^{-1}\left(\frac{1-x^2/R^2}{1+x^2/R^2}\tan\alpha\right)\right] = \frac{2P}{\pi a z}[f(x) - g(x)] \tag{2}$$

$$\sigma_y(x) = -\frac{2P}{\pi a z}\left[\frac{(1-x^2/R^2)\sin 2\alpha}{1+2(x^2/R^2)\cos 2\alpha + x^4/R^4} + \tan^{-1}\left(\frac{1-x^2/R^2}{1+x^2/R^2}\tan\alpha\right)\right] = -\frac{2P}{\pi a z}[f(x) + g(x)] \tag{3}$$

where x is the distance from the origin along the abscissa, P_0 is the amplitude of the sinusoidal load, ω is the angular frequency of the sinusoidal load, t is time, a is the loading strip width, z is the thickness of the sample and R is the radius of the sample. The horizontal strain, $\varepsilon_x(x, t)$, is expressed:

$$\varepsilon_x(x,t) = \frac{1}{E^*}[\sigma_x(x) - \nu\sigma_y(x)] = \frac{2P_0}{E^*\pi a z}e^{i(\omega t-\varphi)}[(\nu+1)f(x) + (\nu-1)g(x)] \tag{4}$$

where E^* is the dynamic modulus, φ is the phase angle and ν is the Poisson's ratio. The total deformation between $-R$ and R at the horizontal central axis, $\Delta H(t)$, is given:

$$\Delta H(t) = \int_{-R}^{R}\varepsilon_x(x,t)dx = \frac{2P_0}{E^*\pi a z}e^{i(\omega t-\varphi)}\left[(\nu+1)\int_{-R}^{R}f(x)dx + (\nu-1)\int_{-R}^{R}g(x)dx\right] = \frac{2P_0}{E^*\pi a z}e^{i(\omega t-\varphi)}A \tag{5}$$

Therefore, in the IDT mode, the dynamic modulus from the horizontal deformation can be expressed as:

$$E^* = |E^*|\cdot e^{i\varphi} = \frac{2P_0\sin(\omega t-\varphi)}{\pi a z\Delta H(t)}A \tag{6}$$

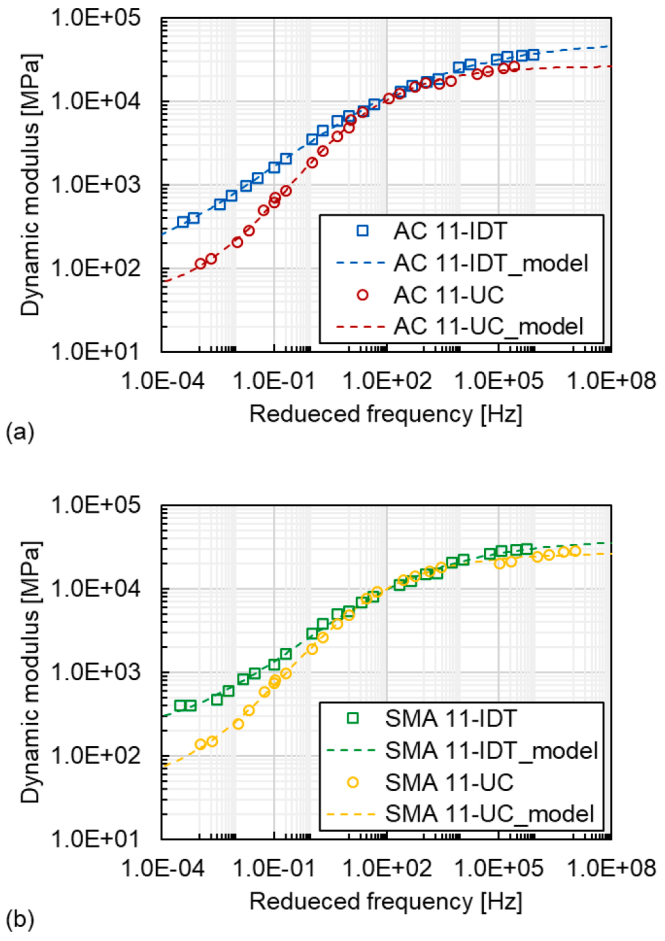

Fig. 8. Master curves of dynamic modulus: (a) AC 11 and (b) SMA 11.

Table 4
The fitting parameters and statistical parameters of the dynamic modulus master curves for asphalt mixtures.

Fitting parameter		AC 11-IDT	SMA 11-IDT	AC 11-UC	SMA 11-UC
Sigmoidal function	δ	1.755	2.152	1.594	1.575
	α	2.974	2.431	2.823	2.847
	β	−0.382	−0.106	−0.385	−0.432
	γ	0.413	0.504	0.701	0.650
WLF equation	C_1	33.802	49.893	19.297	11.018
	C_2	243.539	356.001	166.369	87.622
Goodness of fit statistics					
S_e		724.649	673.983	798.555	1098.795
S_y		12566.958	10345.098	8937.466	10067.358
S_e/S_y		0.058	0.065	0.089	0.109
R^2		0.997	0.996	0.992	0.988

where $|E^*|$ is the norm of the dynamic modulus.

The schematic trend of the stress–strain state for the IDT test is shown in Fig. 3. In the IDT test mode, the value of biaxial stress and strain in the horizontal direction were recorded. The peak-to-peak stress and strain of the specified five cycles per test condition according to EN 12697–26 [30] are used to determine the dynamic modulus. For the cyclic IDT test, the vertical load and the peak-to-peak deformation were recorded to calculate the dynamic modulus based on Eq. (6). The test data is analysed to obtain the dynamic modulus of the IDT test specimen under a certain test condition. The strain response lags to the stress due to the viscoelastic behaviour of asphalt materials, as shown in Fig. 3. The phase angle is to describe the lag of the strain response, which is equal to the lag time, t_{lag}, multiplied by the angular frequency. The stress and strain as a function of the time are expressed in Eq. (7) and Eq. (8).

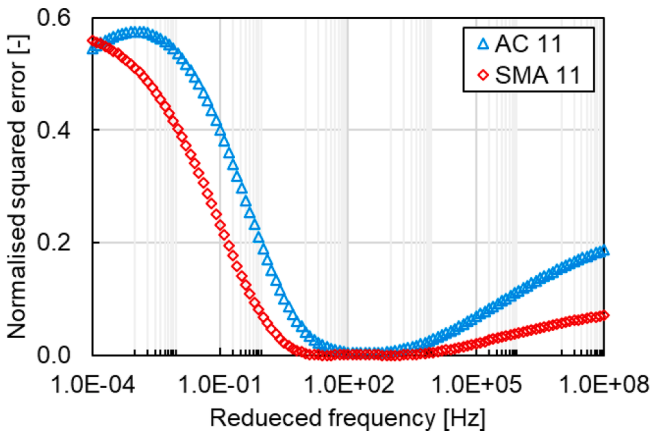

Fig. 9. *NSE* of dynamic modulus between two test modes for AC 11 and SMA 11.

$$\varepsilon(t) = \varepsilon_0 \sin(\omega t) \tag{7}$$

$$\sigma(t) = \sigma_0 \sin(\omega t - \varphi) \tag{8}$$

where σ_0 is the stress amplitude, and ε_0 is the strain amplitude.

2.3.2. Uniaxial compression test

The UC test was performed using the servo-hydraulic UTM (UTM-130) manufactured by IPC global®. The machine is capable of exerting sinusoidal axial load over a wide range of frequencies. Three LVDT with 70 mm gauge lengths installed at 120°apart were used. The test was conducted in accordance with AASHTO T378-17 [34] at the same test conditions as the IDT test. The UC dynamic modulus test was performed in a controlled-strain mode with a target strain of 50 με or less.

The illustration of the UC test is shown in Fig. 4. Differently from the IDT test, the UC test determines the dynamic modulus uniaxially as it measures the vertical stress, $\sigma_y(t)$, and strain, $\varepsilon_y(t)$, along the direction of the applied load as shown in Fig. 5., which is expressed as follows.

$$E^* = |E^*| \cdot e^{i\varphi} = \frac{\sigma_y(t)}{\varepsilon_y(t)} = \frac{\sigma_0 \sin(\omega t - \varphi)}{\varepsilon_0 \sin(\omega t)} \tag{9}$$

In the UC test, the value of axial stress and strain were recorded. The mean value of stiffness from the 10 testing cycles determined the dynamic modulus of the UC test specimen at a certain test condition. As the same as the IDT test, the phase angle can be determined by the lag time between stress and strain.

2.4. Master curve construction

The master curve was constructed by fitting the experimental test data of dynamic modulus according to the sigmoidal function described in the ME pavement design guide was selected as expressed in Eq. (10) and Eq. (11). The WLF equation given in Eq. (12) was used to describe the relationship between shift factor and temperature above the glass transition temperature (T_g) [35].

$$\log(|E^*|) = \delta + \frac{\alpha}{1 + e^{\beta - \gamma(\log f_r)}} \tag{10}$$

$$\log(f_r) = \log(f) + \log[\alpha(T)] \tag{11}$$

where f_r is the frequency at the reference temperature, T_r, T is the test temperature, $\alpha(T)$ is the shift factor, δ, α, β and γ are the fitting parameters.

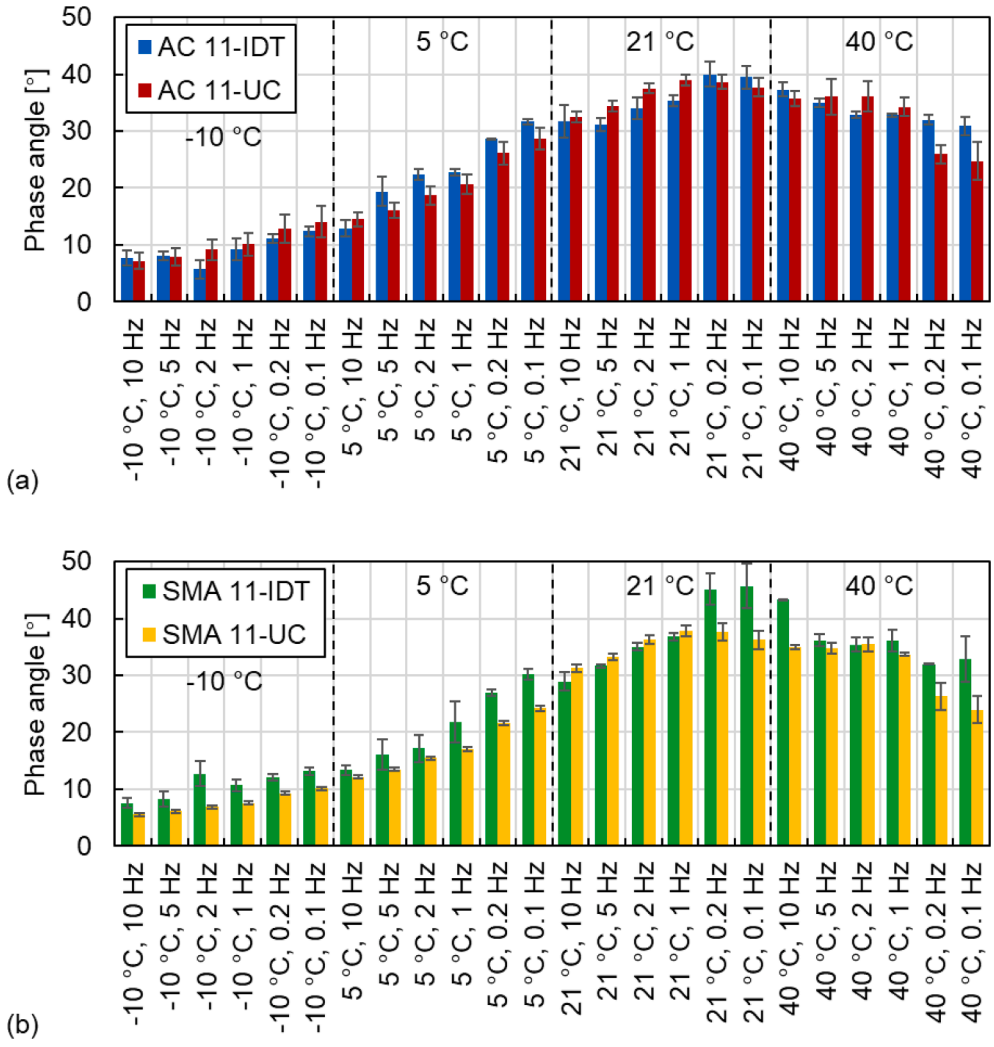

Fig. 10. Phase angle results: (a) AC 11 and (b) SMA 11.

$$\log[\alpha(T)] = \frac{-C_1(T - T_r)}{C_2 + (T - T_r)} \tag{12}$$

where C_1 and C_2 are the fitting parameters. The reference temperature of master curve construction for both tests was the same at 21 °C.

The phase angle master curve was constructed through the Lorentzian equation, denoted as Eq. (13) [36,37]:

$$\varphi = \frac{k_p \cdot k_g^2}{[\log(f_r) - k_c]^2 + k_g^2} \tag{13}$$

where φ is the phase angle, k_p is the peak value, k_g is the growth rate and k_c is the critical point. The master curves of both tests were constructed using the Solver add-in tool in Microsoft Excel. The non-linear least squares regression was performed to fit the test data based on the sigmoidal function, WLF equation and Lorentzian equation [38,39].

3. Results and discussion

3.1. Master curve of dynamic modulus and phase angle

3.1.1. Dynamic modulus

The dynamic modulus results of the IDT and the UC tests are shown in Fig. 6. Fig. 6(a) displays that the dynamic moduli of AC 11 mixtures measured by both tests are similar at 5 °C and there are some differences at higher and lower temperatures. The dynamic moduli of SMA 11 mixtures obtained by two tests are similar at low temperatures (-10 and 5 °C) and different at higher temperatures. The Coefficients of Variation (*CoV*) of the dynamic modulus results are given in Fig. 7. The *CoV* of AC 11-IDT, AC 11-UC, SMA 11-IDT and SMA 11-UC are smaller at −10, 5, 21 °C, which are around 10 % or less. The *CoV* of AC 11-IDT, SMA 11-IDT and SMA 11-UC are bigger at 40 °C, which is up to 30 %. This indicates that the dynamic modulus test has a smaller variation at low temperatures and a bigger variation at high temperatures. Furthermore, the *CoV* of SMA 11 mixtures are lower than the ones of AC 11 mixtures, which displays that the grading type of mixtures has an influence on the test variation.

To compare the two test methods under a wider range of conditions, dynamic modulus master curves of asphalt mixtures are constructed. The dynamic modulus master curves of AC 11-IDT, SMA 11-IDT, AC 11-UC and SMA 11-UC are presented in Fig. 8. The fitting parameters and the goodness of fit statistics [40], including the standard error of estimation (S_e), the standard error of deviation (S_y), the standard error ratio (S_e/S_y) and the coefficients of determination (R^2), are given in Table 4. All master curves have good fits. The R^2 of dynamic modulus are over 0.988. Both R^2 of dynamic modulus for AC 11-IDT and SMA 11-IDT are bigger than the R^2 values of AC 11-UC and SMA 11-UC. Meanwhile, both the S_e/S_y of dynamic modulus for AC 11-IDT and SMA 11-IDT are smaller than the S_e/S_y of AC 11-UC and SMA 11-UC. These outcomes

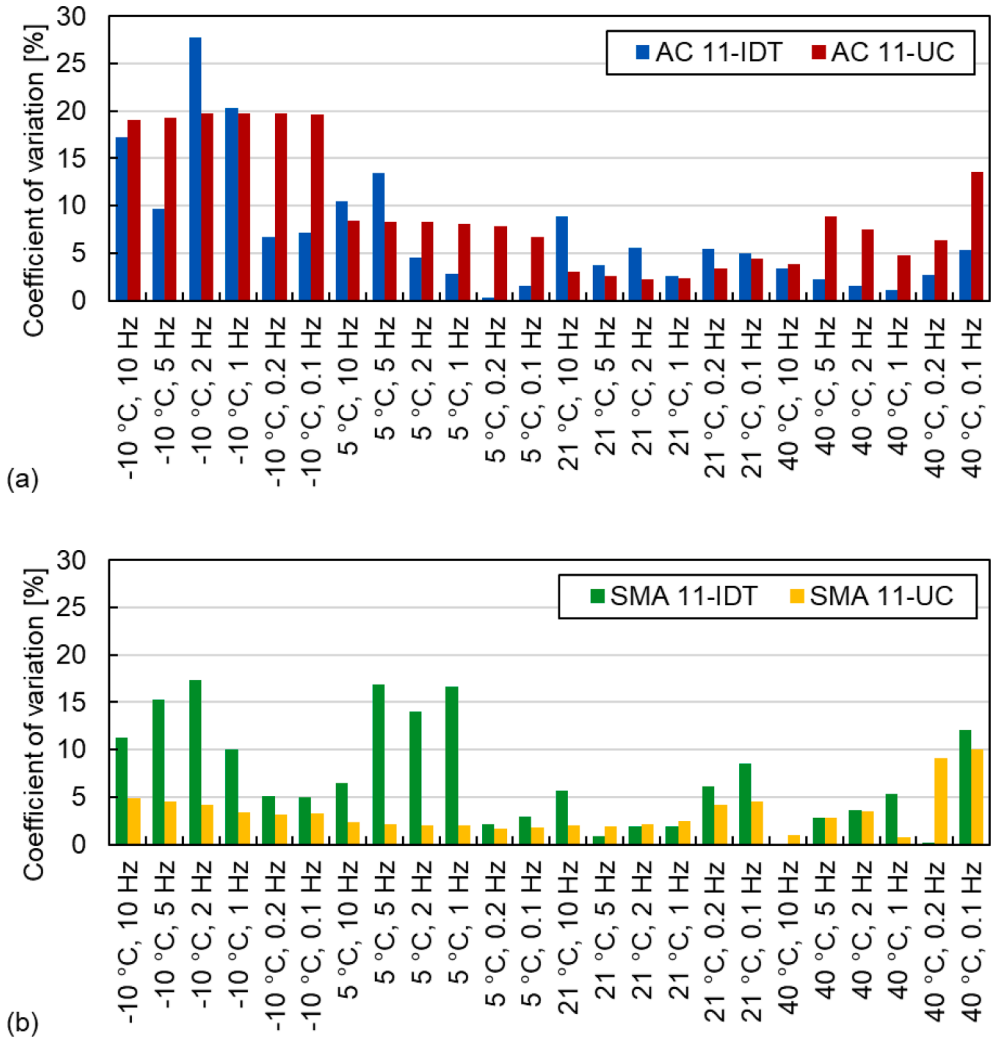

Fig. 11. Coefficient of variation of phase angle results: (a) AC 11 and (b) SMA 11.

indicate that the dynamic modulus master curves have a better fit for IDT test data. Furthermore, it can be observed from Fig. 8 that the dynamic moduli obtained by the two tests are relatively consistent in the frequency range from 10 Hz to 10^4 Hz. When the frequency is higher than 10^4 Hz or lower than 10 Hz, the dynamic moduli display differences. Compared with SMA 11, two tests induce a more severe difference in dynamic modulus at both higher and lower frequencies for AC 11. This result indicates that AC 11 structure tends to expand the difference in dynamic modulus caused by the two tests compared to SMA 11 structure.

As all the dynamic modulus master curves of the four asphalt mixtures have a good fit, the dynamic modulus predicted by the master curves at each frequency is compared by the Normalized Squared Error (*NSE*) following Eq. (14). The smaller the *NSE* value, the more consistent the two test results.

$$NSE = \frac{\left(|E^*|_{IDT} - |E^*|_{UC}\right)^2}{|E^*|_{IDT}^2} \tag{14}$$

where $|E^*|_{IDT}$ is the dynamic modulus obtained by the IDT test, $|E^*|_{UC}$ is the dynamic modulus obtained by the UC test. The *NSE* between two tests of AC 11 and SMA 11 is illustrated in Fig. 9. The dynamic moduli obtained by the two tests are considered relatively consistent with a *NSE* less than 0.005.

As presented in Fig. 9, the dynamic moduli obtained from both tests for the AC 11 are consistent in the frequency range from 10^2 Hz to 10^3 Hz. The dynamic modulus evaluated from both tests for the SMA 11 is consistent in the frequency range from 10 Hz to 10^4 Hz. Meanwhile, the *NSE* of the two mixtures increase gradually with the increase of the frequency over 10^4 Hz or decrease of the frequency less than 10 Hz. The *NSE* of SMA 11 is smaller than that of the *NSE* of AC 11. These results indicate that the dynamic moduli of asphalt mixtures measured by the two tests are almost the same in the reduced frequency range from 10 Hz to 10^4 Hz. On the contrary, differences are found at high and low frequencies (temperatures) where the dynamic moduli measured by the IDT test are greater than those obtained with UC test. Fig. 9 shows that the *NSE* of the two mixtures is large at extreme frequencies, particularly at very low reduced frequencies. This might be connected to the various stress–strain responses of the specimens under the two test modes at relatively high temperatures. The difference in *NSE* between the two asphalt mixtures might be caused by the distinct physical structures. Comparing with AC 11 mixture, SMA 11 has an embedded structure between large size aggregates and its dynamic modulus is less affected by temperature [41].

3.1.2. Phase angle

Fig. 10 presents the phase angle results of the IDT test and the UC test. The phase angles obtained by both tests are similar at 21 °C for AC 11 and SMA 11 mixtures. The differences in phase angles between the

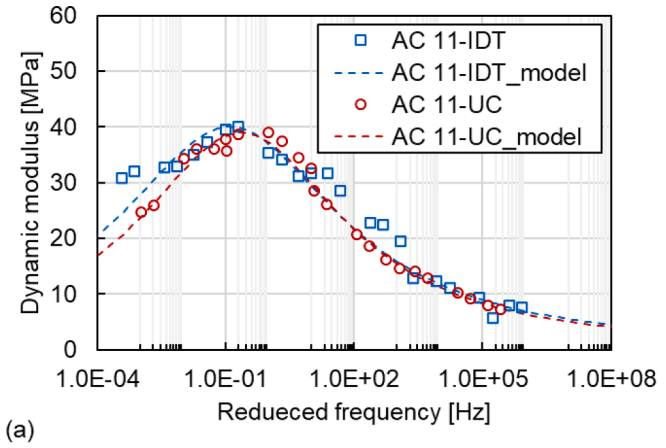

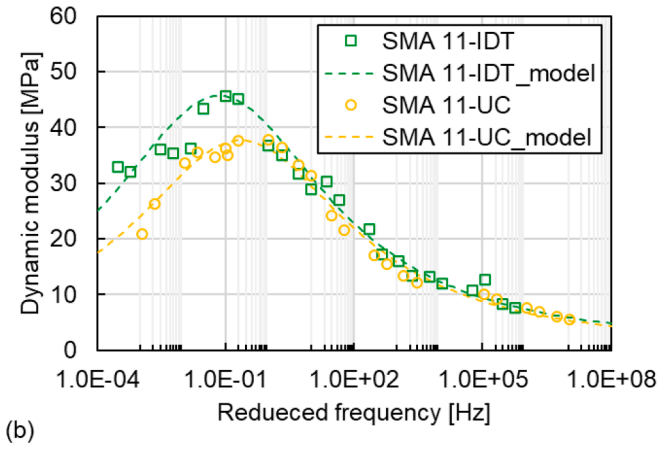

Fig. 12. Master curves of phase angle: (a) AC 11 and (b) SMA 11.

Table 5
The fitting parameters and statistical parameters of the phase angle master curves for asphalt mixtures.

Fitting parameter		AC 11-IDT	SMA 11-IDT	AC 11-UC	SMA 11-UC
Lorentzian equation	k_p	40.006	45.656	38.960	37.745
	k_g	3.167	3.141	2.946	3.114
	k_c	−0.910	−1.154	−0.639	−0.653
Goodness of fit statistics					
S_e		2.961	2.661	1.299	1.611
S_y		11.358	12.273	11.223	11.934
S_e/S_y		0.261	0.217	0.116	0.135
R^2		0.932	0.953	0.987	0.982

two tests occur at higher and lower temperatures. The *CoV* of phase angle results are smaller at 21 °C as shown in Fig. 11, which indicates that the two test modes are stable at 21 °C leading to fewer result differences of both tests in the properties of the same materials.

Similar to the dynamic modulus, phase angle master curves are constructed to compare the differences between the two test methods over a wider range of conditions. The phase angle master curves of AC 11-IDT, SMA 11-IDT, AC 11-UC and SMA 11-UC are presented in Fig. 12. The fitting parameters and the goodness of fit statistics are given in Table 5. The statistical parameters of phase angle for the two tests are different from the ones of dynamic modulus. Both R^2 of phase angle for AC 11-IDT and SMA 11-IDT are smaller than R^2 of AC 11-UC and SMA 11-UC shown in Table 5. Both S_e/S_y of phase angle for AC 11-IDT and SMA 11-IDT exceed S_e/S_y of AC 11-UC and SMA 11-UC. Thus, the phase

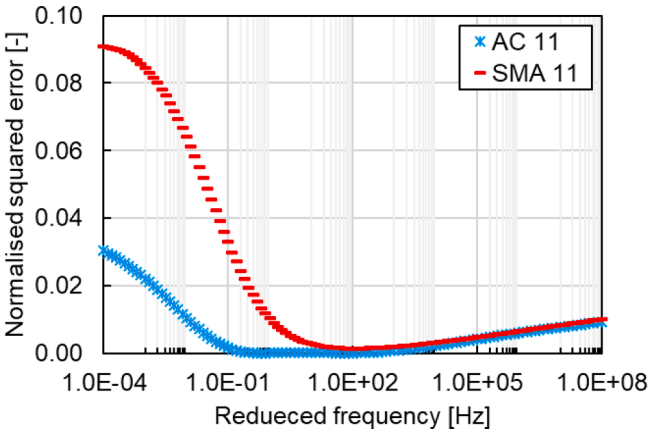

Fig. 13. *NSE* of phase angle between two test modes for AC 11 and SMA 11.

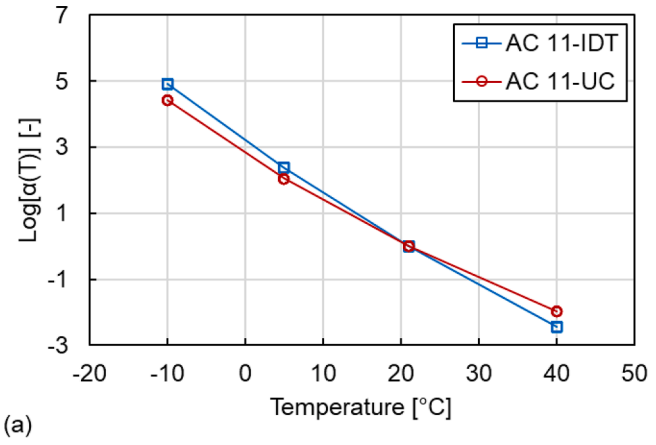

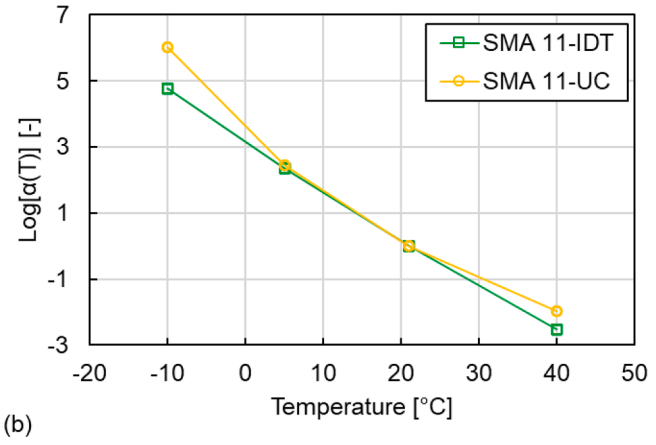

Fig. 14. Shift factors for specimens: (a) AC 11 and (b) SMA 11.

angle master curves of the UC test data have a better fit than that of the IDT test data. As shown in Fig. 12, the phase angle master curves for both tests are similar at high frequencies and show differences at lower frequencies. This difference is more severe for the SMA 11 mixtures than for the AC 11 mixtures.

The *NSE* of the phase angle is calculated from the Lorentzian equation and is also utilised to compare the phase angle at each frequency as similar to the comparison of dynamic modulus. Fig. 13 presents the *NSE* of phase angle for AC 11 and SMA 11. A smaller *NSE* value is obtained at a higher frequency and a bigger *NSE* value emerged at a lower

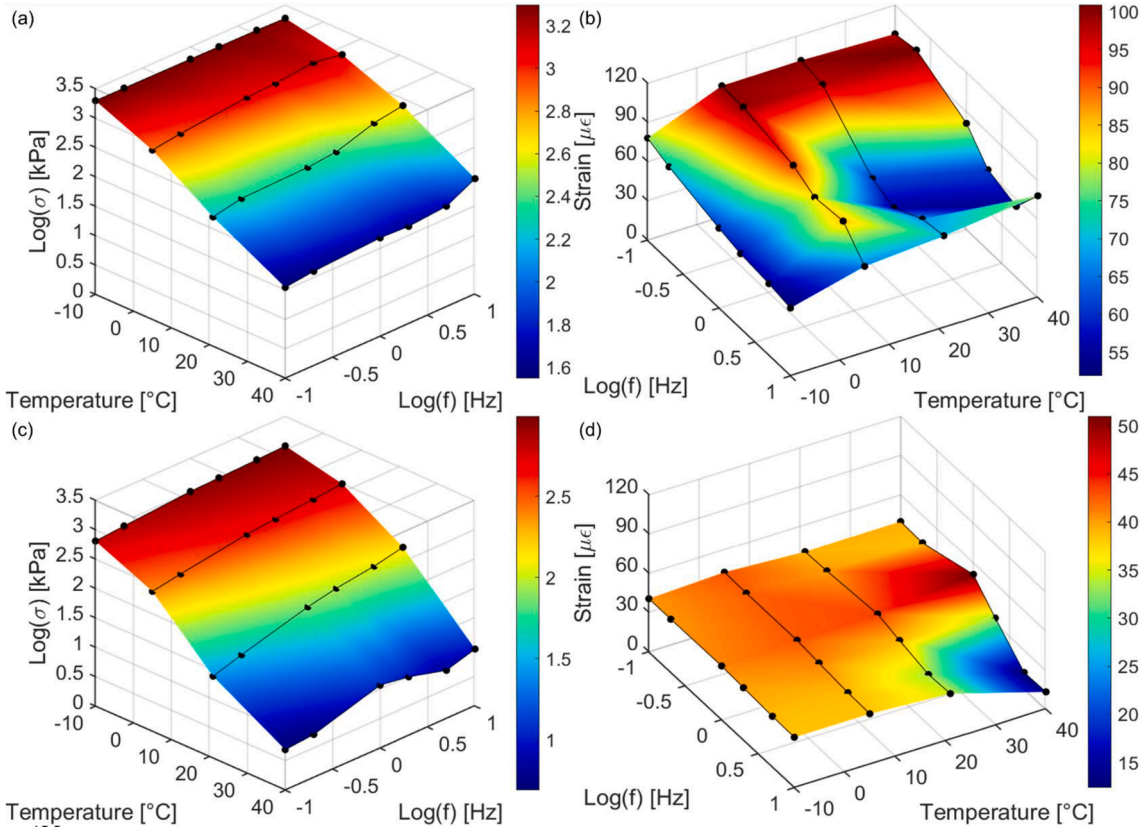

Fig. 15. Stress–strain states of AC 11 in IDT test and UC test at various conditions: (a) AC 11-IDT stress, (b) AC 11-IDT strain, (c) AC 11-UC stress and (d) AC 11-UC strain.

frequency. Meanwhile, the *NSE* of AC 11 is less than 0.005 in the range of 0.1 Hz to 10^5 Hz, showing the consistency of the phase angle of the two tests in this range. For the SMA 11 mixtures, the consistent range of phase angles from 10 Hz to 10^5 Hz for both tests is smaller than the range for the AC 11 mixtures. Furthermore, the *NSE* values of SMA 11 mixtures are bigger than the ones of AC 11 mixtures in the low frequency range. This phenomenon indicates that the difference in phase angle between the two test methods is larger for SMA 11 mixtures than for AC 11 mixtures. Besides, the phase angle of the IDT test is larger than that of the UC test, which is consistent with Kim's research [18]. The horizontal phase angles of the IDT test are generally higher than the phase angles determined from the UC test. The averaged phase angles from horizontal direction and vertical direction are close to the values from the UC test. It can be interpreted that the IDT test only considers the phase angle in the horizontal direction.

3.1.3. Shift factor

The results of the shift factor are also investigated, as shown in Fig. 14. The shift factor reflects how far the measured values have moved relative to the dynamic modulus at the reference temperature, resulting in an impact on the modelling values of the master curves. In terms of AC 11 mixtures, the slope of the shift factor of AC 11-IDT is higher than the one of AC 11-UC, which means that the curve of AC 11-IDT is shifted more in the construction of the master curve than that of AC 11-UC. However, for the SMA 11 mixtures, the measured values of SMA 11-UC move more at high frequencies relative to SMA 11-IDT. When the measured values are higher, moving more distance to high and low frequencies widens the difference, reflecting that the difference in dynamic modulus of the two test methods is greater for the AC 11 mixtures than for the SMA 11 mixtures. This result reveals that the structure of the tested asphalt mixture has a great impact on the results obtained with the two test procedures. The SMA mixtures with the embedded structure are less affected by the test than the AC mixtures with the dense structure.

3.2. Comparison of stress–strain state

3.2.1. Stress–strain response

The stress–strain states are obtained based on Section 2.3. The stress amplitude of the IDT test is expressed in Eq. (15). The stress amplitude of the UC test and the strain amplitudes of the two tests can be obtained from the testing programs.

$$\begin{aligned}\sigma_0 &= \sigma_{0x} - \nu\sigma_{0y} \\ &= \frac{2P_0}{\pi az}(\sin 2\alpha - \alpha) - \nu\left[-\frac{2P_0}{\pi az}(\sin 2\alpha + \alpha)\right] \\ &\approx \frac{P_0}{\pi Rz} + \nu\frac{3P_0}{\pi Rz}\end{aligned} \tag{15}$$

The stress–strain states of AC 11 mixtures for the two tests are represented in Fig. 15 at various temperature and frequency conditions. Fig. 16 shows the *CoV* of the stress and strain results. As shown in Fig. 15 (a, c), the stresses of both test modes for AC 11 decrease as the temperature increases. This is explained that both test modes control the strain in a certain range to ensure that the tested asphalt mixture is in the linear viscoelastic range. The increase in temperature causes the softening of the asphalt mixture yet the strain range does not change. The strains of two tests for AC 11 are shown in Fig. 15(b, d). It is observed

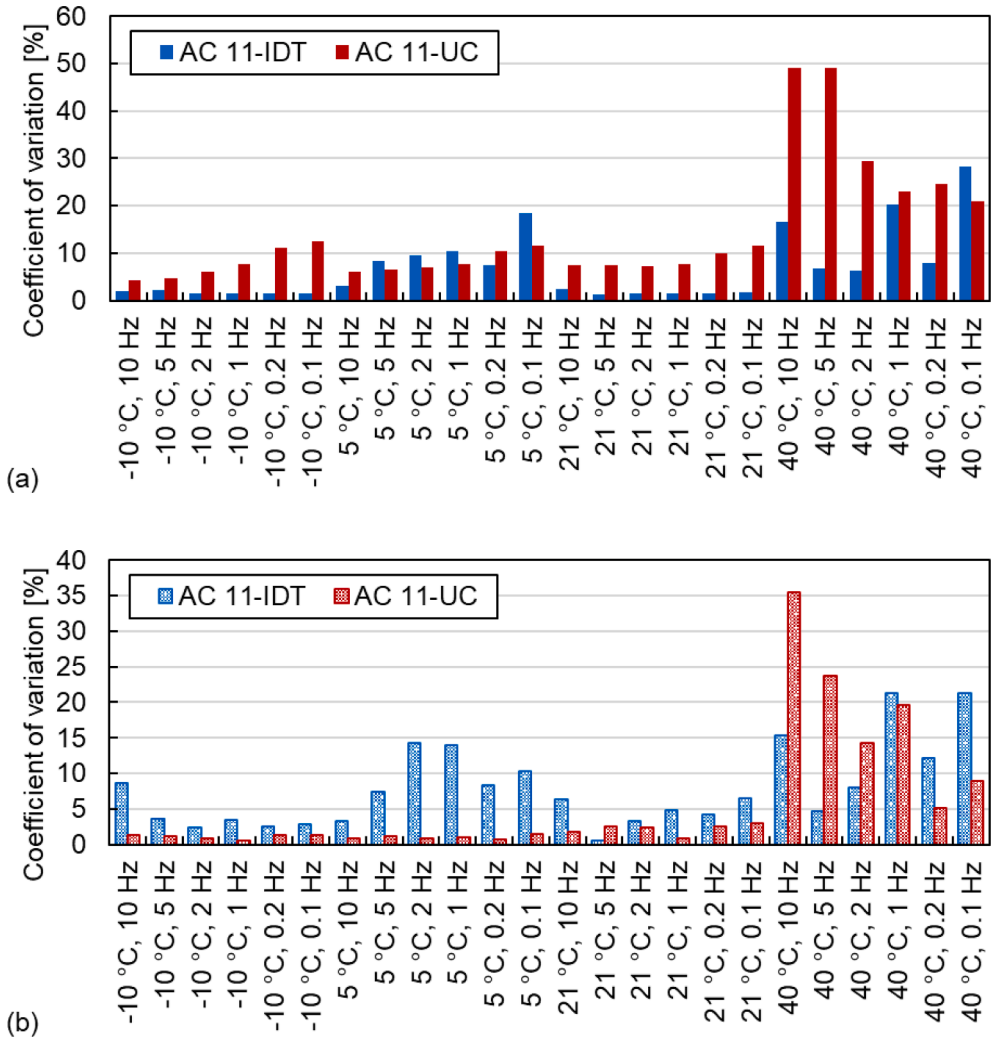

Fig. 16. Coefficient of variation of stress and strain results of AC 11 mixtures: (a) stress and (b) strain.

that the strains of the UC test are maintained around 40 με at all temperatures except for 40 °C. However, the strains of the IDT test are not stable at a certain value with the temperature changing, and there is no intuitive changing trend between the strain and the temperature. This indicates that the UC test controls the strain better than the IDT test and the strains of both tests are varied at the high temperatures.

Fig. 15 also shows the changes in stress and strain with the frequency. At low temperatures, the stresses measured for both tests are maintained at a relatively constant stress level as the frequency changes. The stresses are gradually affected by frequency as the temperature increases. For high temperatures, the stress values fluctuate more with various frequencies for both tests. The variation in the trends of strain and stress with frequency for the IDT test is similar, while the strain in the UC test is stable at an average of 40 με. When it comes to the changes in strains, the UC test has better deformation control than the IDT test. However, both approaches do not control the deformation well at high temperatures due to the viscous properties of the asphalt mixture at high temperatures. The change in the stress–strain state with temperature and frequency can be explained by considering the viscoelastic behaviour of asphalt materials. At low temperatures, the elastic component plays a major role; therefore, the dynamic modulus does not change much with frequency, and the stress and strain are stable. At high temperatures, the viscous component plays a more important role, and the dynamic modulus as well as the stress–strain state are highly related to temperature values. It is worth noting that the strain value measured during the IDT test at a high temperature and low frequency is close to the upper limit. Therefore, it is difficult to ensure that the asphalt material specimen is within the linear viscoelastic range at high temperatures when investigated with the IDT test.

Fig. 16 indicates that the *CoV* of stress and strain results for AC 11 mixtures are small at −10, 5, 21 °C and high at 40 °C, which is consistent with the *CoV* of dynamic modulus results. This result further reflects that the mechanical properties of asphalt mixtures are more stably determined at low and medium temperatures by both two test modes. The larger variations occur at high temperatures.

The stress–strain states measured for SMA 11 mixtures and their *CoV* are shown in Fig. 17 and Fig. 18, respectively. The trend of stress–strain states for SMA 11 is similar to the one for AC 11, indicating the major relevance of the viscoelastic properties of asphalt materials. However, there are still some distinctions between the two asphalt mixtures. At low temperatures, the stress of the SMA 11 is larger than that of the AC 11 except for 10 Hz in the IDT test. The strain of the SMA 11 is bigger than that of the AC 11 except for 10 Hz in the IDT test. Meanwhile, the stresses of the UC test grow slowly with the increase in frequency, and

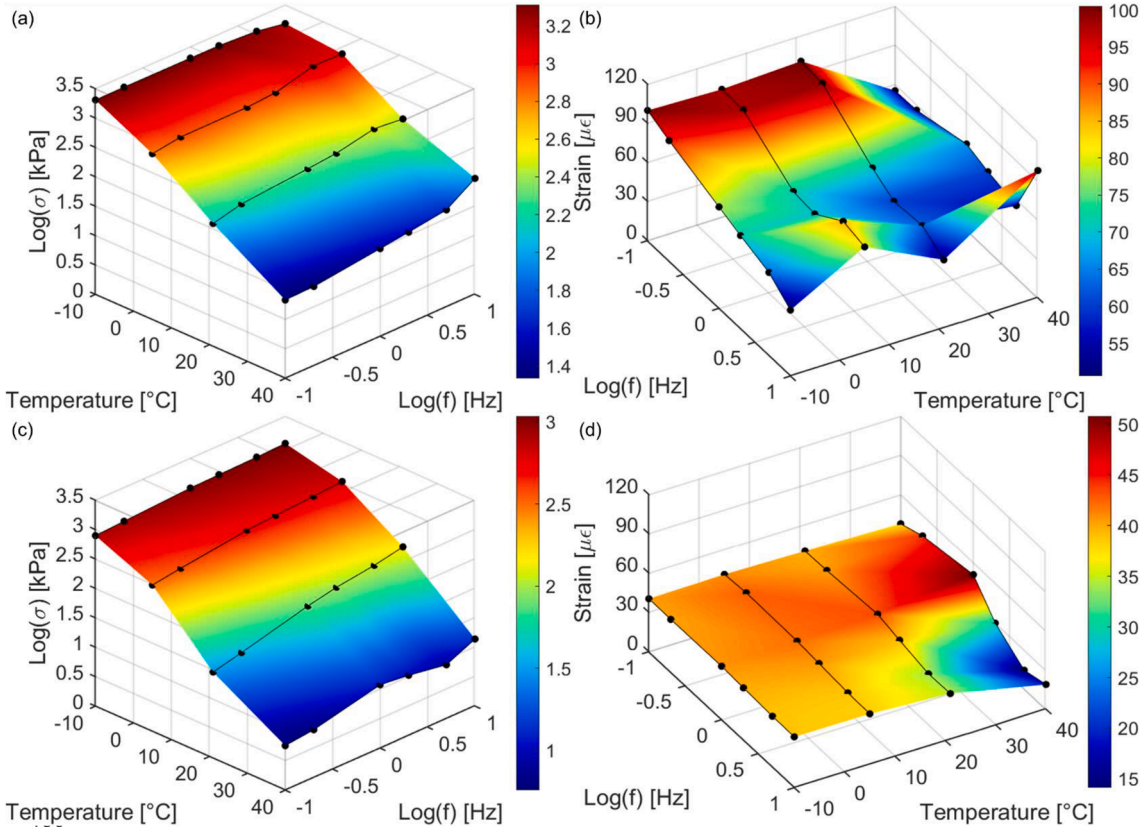

Fig. 17. Stress–strain states of SMA 11 in IDT test and UC test at various conditions: (a) SMA 11-IDT stress, (b) SMA 11-IDT strain, (c) SMA 11-UC stress and (d) SMA 11-UC strain.

the strains remain around 40 με for both AC 11 and SMA 11. Thus, this finding illustrates that the UC test has better control of stress and strain than the IDT test. Comparing the results depicted in Fig. 15(a, c) and Fig. 17(a, c) for high temperatures, the IDT test stress values measured for the SMA 11 samples are smaller than the ones for the AC 11 specimens. At 40 °C, the stress values of the SMA 11 in the IDT test decrease on average by about 15 % relative to the AC 11. However, the stress of the SMA 11 is almost the same as that of the AC 11 in the UC test at 40 °C. The trends of the strain values measured for both SMA 11 and AC 11 asphalt mixtures are similar at high temperatures.

The *CoV* of stress and strain results for SMA 11 mixtures have a similar trend to that for AC 11 mixtures as presented in Fig. 18. It is worth finding that the *CoV* of the UC test strain is very small at −10, 5, 21 °C and is relatively large at 40 °C for both asphalt mixtures. This reflects that the UC test has a very stable control on strain at −10, 5, 21 °C and controls strain unstably at high temperatures.

3.2.2. Normalised stress and strain

As the different modes of control strain for the two tests, the stress and the strain are normalised by dividing by the maximum value method for comparison. The normalised stresses at every temperature are used to reflect the changing trend of the stress. The exponential formulations used to fit the experimental values of mean stress and temperature are shown in Fig. 19. The high R^2 values validate the reliability of the relationship. The normalised stresses at −10 °C are similar for both tests and the difference occurs at high temperatures. At 40 °C, the values of normalised stresses measured by the IDT test are approximately 3.26 and 2.34 times greater than the ones measured by the UC test for AC 11 and SMA 11 mixtures, respectively. Compared with UC test, the results indicate that the stress level of the IDT test is higher and the difference between the two tests of AC 11 is greater than that of SMA 11 in terms of stress.

The relationship between normalised strain and temperature is shown in Fig. 20. At −10 °C, the normalized strain of the UC test has a stable value of around 0.8, which corresponded to 40 με. The strain difference with frequencies increases gradually with the increase in temperature. At 40 °C, the strains of the UC test at six frequencies are quite different. The normalised strain of the IDT test shows large deviations at all four test temperatures. The strain deviation under different frequencies of the IDT test is greater than that of the UC test at −10, 5 and 21 °C and smaller than that of the UC test at 40 °C. The results indicate that the changing trend of strain with temperature for the UC test is smaller than that of the IDT test at low and medium temperatures, while higher at high temperatures. This result demonstrates a better control over strain of the UC test at low and medium temperatures, which is consistent with the *CoV* of strain results.

3.3. Comparison between IDT test and UC test

The main features of the IDT test and UC test setups and result trends are summarised in Table 6. Due to the smaller dimension (weight) of the test specimen dimension (weight) the IDT test is more convenient for testing field core samples and for sample preparation in the laboratory, e.g., making plate samples and core and cut from them. The biaxial stress of the IDT test involves Poisson's ratio. In this test, the stress–strain response in horizontal direction is only considered and Poisson's ratio is

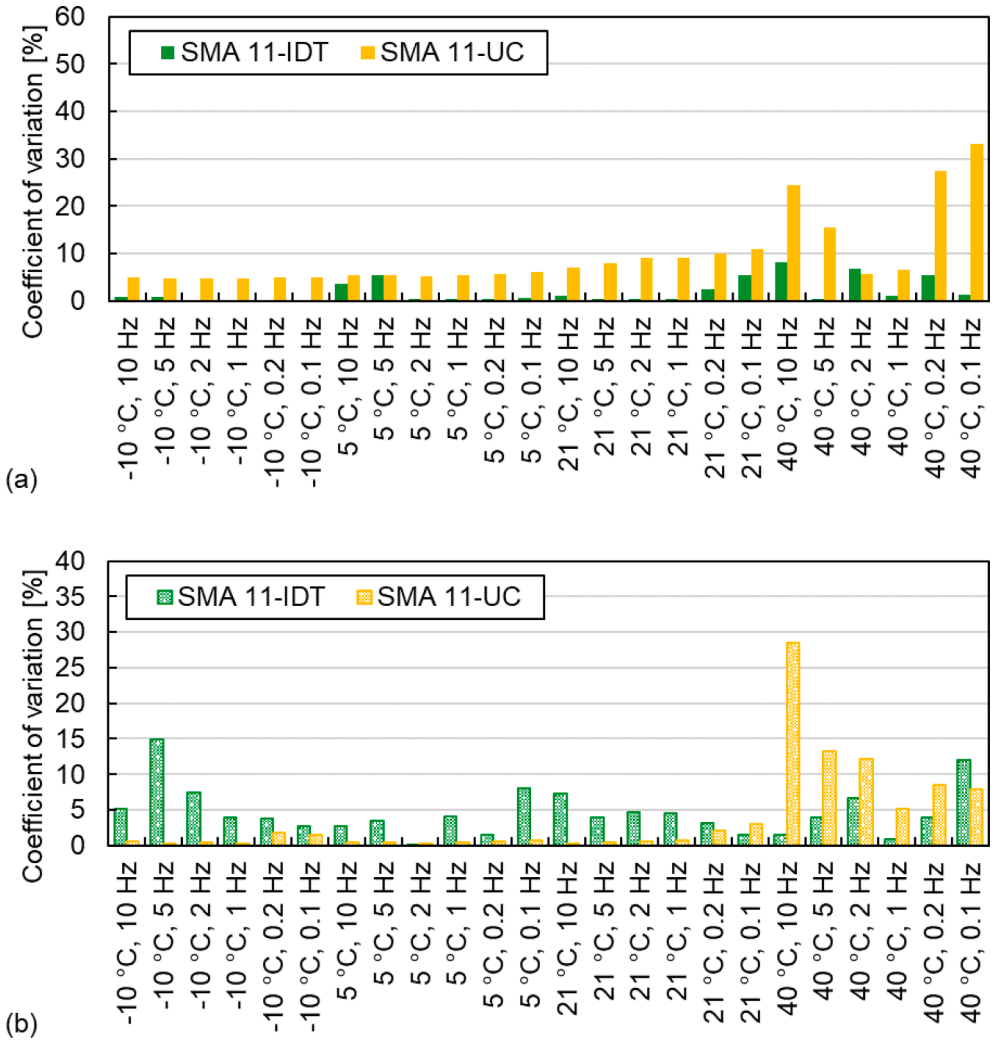

Fig. 18. Coefficient of variation of stress and strain results of SMA 11 mixtures: (a) stress and (b) strain.

selected as a constant value of 0.35 according to the standard (EN 12697–26). Differently from IDT test, the UC test takes account into stresses in a single direction (vertical direction) less affected by Poisson's ratio. Moreover, the UC test employs confining pressure, which can better simulate real service conditions of road pavement [42]. However, the UC test needs more time to condition temperature due to the larger size of the sample. Nevertheless, both IDT test and UC test can work well at intermediate temperatures. Considering the dynamic moduli, the results from the two tests are almost identical for intermediate frequency and temperature ranges, and slightly different at extreme temperatures. Regarding the phase angle, the UC test results are more accurate than IDT test results. Besides, the stress–strain states for IDT test and UC test are different. This is due to the different force forms and strain control modes of the two tests. The biaxial and uniaxial loads are applied to the IDT and UC tests, respectively. The initial strain of IDT test is controlled manually, while the strain of UC test is controlled by the software in the whole test procedure. Furthermore, the greater number of analysed cycles for the UC test also reflects better stability than the IDT test. Therefore, the UC test shows better deformation control at low and medium temperatures.

4. Conclusions

This study compares the two standard laboratory tests used for the mechanical characterisation of bituminous asphalt, namely Indirect Tensile (IDT) test and Uniaxial Compression (UC). The performance of two mixtures commonly employed for road surfacing, Asphalt Concrete (AC) and Stone Mastic Asphalt (SMA), are compared in terms of dynamic modulus, phase angle, shift factor and stress–strain state. Based on the attained results, the conclusions are drawn as follows:

- The dynamic moduli measured using both tests at medium frequency (temperature) range are the same. Moreover, the values obtained from IDT test are higher than the ones assessed by UC test at extreme frequencies (temperatures). The different mesoscopic structures of the asphalt mixture can account for the discrepancies in the results attained with the two test methods. The difference in dynamic modulus of SMA mixtures measured by both tests is smaller than that of AC mixtures.
- Compared with IDT test, the phase angle master curve has a better fit for UC test and has lower values.
- The shift factor of SMA 11-UC is bigger than that of SMA 11-IDT at low temperatures, which is different from the situation for AC 11

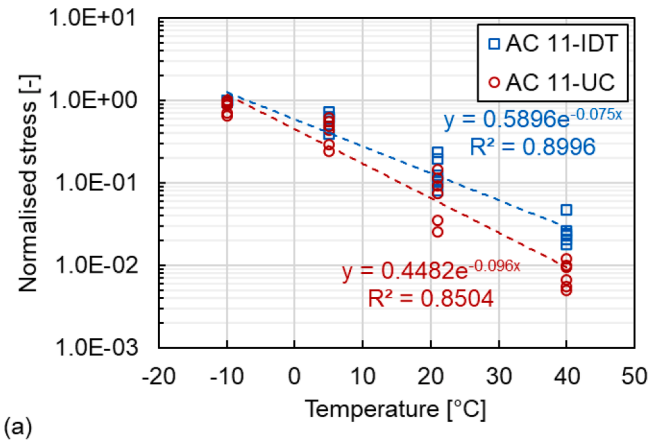

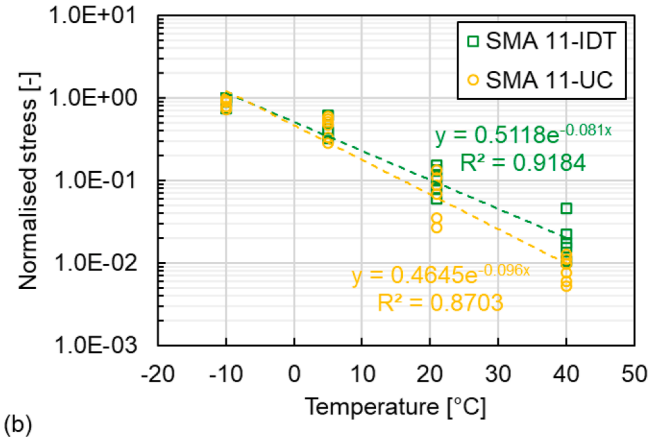

Fig. 19. Relationship between normalised stress and temperature: (a) AC 11 and (b) SMA 11.

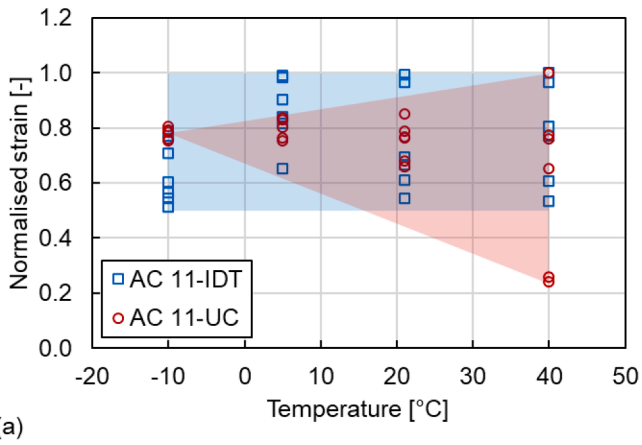

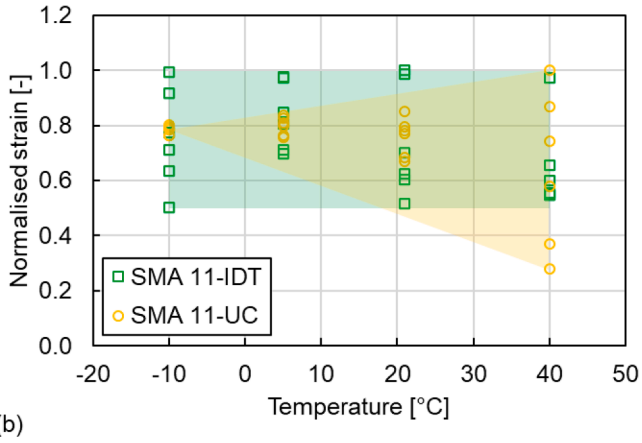

Fig. 20. Relationship between normalised strain and temperature: (a) AC 11 and (b) SMA 11.

mixtures. The measured dynamic modulus and the shifting situation cause a smaller difference between the two test methods in modelling dynamic modulus for the SMA 11 mixtures.

- The stress level pertaining to the IDT test is bigger than the one achieved during UC test. The IDT test strain values are various at all four test temperatures. Although the variation of strain obtained from the UC test is based on the frequency largens as the temperature increases, the stress–strain states are stable at low and medium temperatures, showing a better strain control than the IDT test.
- The coefficients of variation of dynamic modulus, stress and strain results are small at −10, 5, 21 °C and higher at 40 °C indicating that both test modes are more stable for testing the mechanical properties of asphalt mixtures at low and medium temperatures. The phase angle results only show small variations at 21 °C.

In general, both tests can be used to properly characterise the dynamic modulus of asphalt materials. The IDT test can be efficiently used for the characterisation of road surfaces built in cold regions. Moreover, the IDT test plays an important role when it comes to the mechanical characterisation of existing asphalt pavements since the dimensions of the field samples normally meet the size requirements. The UC test controls strain better for low and medium temperature ranges compared with IDT test, resulting in more accurate results. A confining pressure can be applied for UC test, which better simulates real field conditions. For Norwegian conditions as a basis for practical design, the IDT test seems to be the best choice due to easier/more realistic sample preparation and to compare with field cored samples.

The comparison between IDT and UC modes in dynamic modulus tests for AC 11 and SMA 11 mixtures was focused on in this study. Further studies involving more types of asphalt mixtures are recommended to investigate the effect of materials on the difference between the two test modes and fully understand the two modes of dynamic modulus tests. Moreover, the connection of the IDT and UC tests under extreme environmental conditions will be established to develop the wide application of the IDT test in ME pavement design.

5. Data availability

Data will be made available on request.

CRediT authorship contribution statement

Hao Chen: Conceptualization, Methodology, Software, Formal analysis, Investigation, Data curation, Writing – original draft. **Mequanent Mulugeta Alamnie:** Conceptualization, Methodology, Investigation, Data curation, Writing – review & editing. **Diego Maria Barbieri:** Investigation, Writing – review & editing. **Xuemei Zhang:** Investigation, Writing – review & editing. **Gang Liu:** Methodology, Writing – review & editing, Supervision. **Inge Hoff:** Resources, Writing – review & editing, Supervision.

Table 6
Summarised comparison between IDT test and UC test.

Item			IDT test	UC test
Standard			EN 12697–26:2018	AASHTO T378-17
Cylindrical specimen dimension	Diameter		100 mm	100 mm
	Thickness (height)		40 mm	150 mm
Conditioning temperature time			≥ 4 h (Better for low temperature)	−10 °C ~ Overnight 5 °C ~ 4 h or Overnight 21 °C ~ 3 h 40 °C ~ 2 h (Suitable for intermediate and high temperature)
Test temperature (this study)			−10 °C, 5 °C, 21 °C, 40 °C	
Test frequency (this study)			10 Hz, 5 Hz, 2 Hz, 1 Hz, 0.2 Hz, 0.1 Hz	
Applied load			Harmonic sinusoidal load	
Load control mode			Controlled stress–strain	Controlled strain
Number of analysed cycles			5 cycles	10 cycles
Dynamic modulus	f_r: 10^{-4} ~ 10 Hz	AC 11	255 ~ 6379 MPa	67 ~ 5072 MPa
		CoV	1.4 % ~ 11.0 %	5.7 % ~ 32.9 %
		SMA 11	292 ~ 5341 MPa	74 ~ 5028 MPa
		CoV	0.2 % ~ 10.6 %	5.7 % ~ 32.3 %
	f_r: 10 ~ 10^4 Hz	AC 11	6379 ~ 24329 MPa	5072 ~ 20224 MPa
		CoV	0.1 % ~ 7.7 %	5.8 % ~ 11.7 %
		SMA 11	5341 ~ 21066 MPa	5028 ~ 19546 MPa
		CoV	0.5 % ~ 8.3 %	5.3 % ~ 6.7 %
	f_r: 10^4 ~ 10^8 Hz	AC 11	24329 ~ 45411 MPa	20224 ~ 25731 MPa
		CoV	1.1 % ~ 3.9 %	4.1 % ~ 6.2 %
		SMA 11	21066 ~ 35123 MPa	19546 ~ 25808 MPa
		CoV	4.0 % ~ 7.5 %	4.8 % ~ 4.9 %
	S_e/S_y	AC 11	0.058	0.089
		SMA 11	0.065	0.109
	R^2	AC 11	0.997	0.992
		SMA 11	0.996	0.988
Phase angle	f_r: 10^{-4} ~ 10 Hz	AC 11	20 ~ 40°	17 ~ 39°
		CoV	1.0 % ~ 5.5 %	2.2 % ~ 13.6 %
		SMA 11	25 ~ 46°	18 ~ 38°
		CoV	0.1 % ~ 12.1 %	0.8 % ~ 10.0 %
	f_r: 10 ~ 10^4 Hz	AC 11	12 ~ 29°	11 ~ 30°
		CoV	0.3 % ~ 13.4 %	3.0 % ~ 19.8 %
		SMA 11	12 ~ 31°	12 ~ 29°
		CoV	2.1 % ~ 16.9 %	1.7 % ~ 2.4 %
	f_r: 10^4 ~ 10^8 Hz	AC 11	4 ~ 12°	4 ~ 11°
		CoV	9.7 % ~ 27.8 %	19.0 % ~ 19.7 %
		SMA 11	5 ~ 12°	4 ~ 11°
		CoV	10.1 % ~ 17.4 %	3.1 % ~ 4.9 %
	S_e/S_y	AC 11	0.261	0.116
		SMA 11	0.217	0.135
	R^2	AC 11	0.932	0.987
		SMA 11	0.953	0.982
Shift factor	$T < T_r$	AC 11	2.4 ~ 4.9	2.0 ~ 4.4
		SMA 11	2.3 ~ 4.8	2.5 ~ 6.0
	$T \geq T_r$	AC 11	−2.4 ~ 0	−2.0 ~ 0
		SMA 11	−2.5 ~ 0	−2.0 ~ 0
Stress	Direction		Horizontal and vertical (biaxial)	Vertical (uniaxial)
	$T < T_r$	AC 11	766 ~ 1982 kPa	240 ~ 987 kPa
		CoV	1.5 % ~ 18.4 %	4.3 % ~ 12.5 %
		SMA 11	665 ~ 2047 kPa	306 ~ 1087 kPa
		CoV	0.1 % ~ 5.5 %	4.7 % ~ 6.2 %
	$T \geq T_r$	AC 11	35 ~ 468 kPa	5 ~ 143 kPa
		CoV	1.2 % ~ 28.3 %	7.3 % ~ 49.2 %
		SMA 11	22 ~ 310 kPa	6 ~ 146 kPa
		CoV	0.3 % ~ 8.3 %	5.6 % ~ 33.2 %
Strain	Direction		Horizontal	Vertical
	$T < T_r$	AC 11	52 ~ 100 με	38 ~ 43 με
		CoV	2.3 % ~ 14.3 %	0.6 % ~ 1.5 %
		SMA 11	51 ~ 100 με	38 ~ 43 με
		CoV	0.1 % ~ 14.9 %	0.3 % ~ 1.8 %
	$T \geq T_r$	AC 11	54 ~ 101 με	12 ~ 51 με
		CoV	0.5 % ~ 21.3 %	0.8 % ~ 35.5 %
		SMA 11	52 ~ 101 με	14 ~ 51 με
		CoV	0.8 % ~ 11.9 %	0.3 % ~ 28.5 %

Declaration of Competing Interest

The authors declare that they have no known competing financial interests or personal relationships that could have appeared to influence the work reported in this paper.

Data availability

Data will be made available on request.

Acknowledgements

This research work was supported by the VegDim project of the Norwegian Public Roads Administration. The financial support provided by China Scholarship Council (No. 201806950077) and Department of Civil and Environmental Engineering, Norwegian University of Science and Technology (No. K-649105) is highly acknowledged. The support kindly provided by the laboratory technicians Bent Lervik and Jan Erik Molde is greatly acknowledged.

References

[1] Y.H. Huang, Pavement analysis and design, Pearson Prentice, Hall Upper Saddle River, NJ, 2004.
[2] A. Maji, A. Das, Reliability considerations of bituminous pavement design by mechanistic–empirical approach, Int. J. Pavement Eng. 9 (1) (2008) 19–31.
[3] Nchrp, Guide for Mechanistic-Empirical Design of New and Rehabilitated Pavement Structures, NCHRP 1–37A Part 2 Design Inputs Chapter 2 Material Characterization, Transportation Research Board, Washington, D.C., 2004.
[4] D. Lesueur, J.F. Gerard, P. Claudy, J.M. Letoffe, J.P. Planche, D. Martin, A structure-related model to describe asphalt linear viscoelasticity, J. Rheol. 40 (5) (1996) 813–836.
[5] D.D. Li, M.L. Greenfield, Viscosity, relaxation time, and dynamics within a model asphalt of larger molecules, J. Chem. Phys. 140 (3) (2014), 034507.
[6] X. Zhang, H. Chen, D.M. Barbieri, B. Lou, I. Hoff, The classification and reutilisation of recycled asphalt pavement binder: Norwegian case study, Case Stud. Constr. Mater. 17 (2022) e01491.
[7] T. Officials, AASHTO Guide for Design of Pavement Structures, AASHTO (1993).

[8] C.W. Schwartz, N. Gibson, R.A. Schapery, Time-temperature superposition for asphalt concrete at large compressive strains, Transp. Res. Rec. 1789 (1) (2002) 101–112.
[9] H. Yao, Z. You, L. Li, C.H. Lee, D. Wingard, Y.K. Yap, X. Shi, S.W. Goh, Rheological properties and chemical bonding of asphalt modified with nanosilica, J. Mater. Civ. Eng. 25 (11) (2013) 1619–1630.
[10] T. Chen, Y. Luan, T. Ma, J. Zhu, X. Huang, S. Ma, Mechanical and microstructural characteristics of different interfaces in cold recycled mixture containing cement and asphalt emulsion, J. Clean. Prod. 258 (2020), 120674.
[11] J. Zhu, T. Ma, J. Fan, Z. Fang, T. Chen, Y. Zhou, Experimental study of high modulus asphalt mixture containing reclaimed asphalt pavement, J. Clean. Prod. 263 (2020), 121447.
[12] D.W. Christensen, R.F. Bonaquist, Evaluation of indirect tensile test (IDT) procedures for low-temperature performance of hot mix asphalt, Transp. Res. Board (2004).
[13] M. Zaumanis, M.C. Cavalli, L.D. Poulikakos, How not to design 100% recycled asphalt mixture using performance-based tests, Road Mater. Pavement Des. 21 (6) (2020) 1634–1646.
[14] K. Mollenhauer, P. Plachkova-Dzhurova, Categories for stiffness and fatigue based on cyclic indirect tensile tests and their applicability in construction contracts. 6th Eurasphlat & Eurobitumen Congress, 2016.
[15] X. Zhang, H. Chen, D.M. Barbieri, I. Hoff, Laboratory Evaluation of Mechanical Properties of Asphalt Mixtures Exposed to Sodium Chloride, 03611981221082579, Transp. Res. Rec. (2022).
[16] R.G. Saba, Analytical Design of Pavement Structures, NPRA reports, Norway, (2019).
[17] H. Cheng, Y. Wang, L. Liu, L. Sun, Y. Zhang, R. Yang, Estimating tensile and compressive moduli of asphalt mixture from indirect tensile and four-point bending tests, ASCE J. Mater. Civ. Eng. 33 (1) (2021) 04020402.
[18] Y.R. Kim, Y. Seo, M. King, M. Momen, Dynamic modulus testing of asphalt concrete in indirect tension mode, Transp. Res. Rec. 1891 (1) (2004) 163–173.
[19] X. Qin, L. Ma, H. Wang, Comparison analysis of dynamic modulus of asphalt mixture: indirect tension and uniaxial compression test, Transportmetrica A 15 (1) (2019) 165–178.
[20] D. Barbieri, I. Hoff, H. Mork, Laboratory investigation on unbound materials used in a highway with premature damage, Bearing capacity of Roads, Railways and Airfields, CRC Press, 2017, pp. 101–108.
[21] D.M. Barbieri, I. Hoff, M.B.E. Mørk, Mechanical assessment of crushed rocks derived from tunnelling operations, in: Civil Infrastructures Confronting Severe Weathers and Climate Changes Conference, Springer, 2018, pp. 225–241.
[22] CEN, EN 1426:2015 Bitumen and bituminous binders Determination of needle penetration, Brussels, Belgium, (2015).
[23] CEN, EN 1427:2015 Bitumen and bituminous binders Determination of the softening point Ring and Ball method, Brussels, Belgium, (2015).
[24] CEN, EN 1097-1:2011 Tests for mechanical and physical properties of aggregates Part 1: Determination of the resistance to wear (micro-Deval), Brussels, Belgium, (2011).
[25] CEN, EN 1097-2:2020 Tests for mechanical and physical properties of aggregates Part 2: Methods for the determination of resistance to fragmentation, Brussels, Belgium, (2020).
[26] CEN, EN 12697-31:2019 Bituminous mixtures Test methods Part 31: Specimen preparation by gyratory compactor, Brussels, Belgium, (2019).
[27] M.M. Alamnie, E. Taddesse, I. Hoff, Thermo-piezo-rheological characterization of asphalt concrete, Constr. Build. Mater. 329 (2022), 127106.
[28] R.E. Asbjørn Arnevik, Nils Sigurd Uthus, Joralf Aurstad, Jostein Aksnes, Torbjørn Jørgensen, Guidelines asphalt 2019, NPRA reports, Norway, (2019).
[29] CEN, EN 12697-8:2018 Bituminous mixtures Test methods Part 8: Determination of void characteristics of bituminous specimens, Brussels, Belgium, (2018).
[30] CEN, EN 12697-26:2018 Bituminous mixtures Test methods Part 26: Stiffness, Brussels, Belgium, (2018).
[31] G. Cerni, E. Bocci, F. Cardone, A. Corradini, Correlation between asphalt mixture stiffness determined through static and dynamic indirect tensile tests, Arab. J. Sci. Eng. 42 (3) (2017) 1295–1303.
[32] F. Olard, F. Noël, F. Loup, Modulus testing in indirect tension mode, Road Mater. Pavement Des. 7 (4) (2006) 543–554.
[33] P. Ghasemi, S. Lin, D.K. Rollins, R.C. Williams, Predicting dynamic modulus of asphalt mixture using data obtained from indirect tension mode of testing, arXiv preprint arXiv:1905.06810 (2019).
[34] AASHTO, T 378-17 Standard Method of Test for Determination the Dynamic Modulus and Flow Number for Asphalt Mixtures Using the Asphalt Mixture Performance Tester (AMPT), Washington, D.C., (2017).
[35] M.L. Williams, R.F. Landel, J.D. Ferry, The temperature dependence of relaxation mechanisms in amorphous polymers and other glass-forming liquids, J. Am. Chem. Soc. 77 (14) (1955) 3701–3707.
[36] R. Nemati, E.V. Dave, Nominal property based predictive models for asphalt mixture complex modulus (dynamic modulus and phase angle), Constr. Build. Mater. 158 (2018) 308–319.
[37] A.R. Archilla, J.P. Corrales-Azofeifa, J.P. Aguiar-Moya, Comprehensive Model for the Prediction of the Phase Angle Master Curve of Asphalt Concrete Mixes, in: RILEM International Symposium on Bituminous Materials, Springer, 2020, pp. 473–479.
[38] T.K. Pellinen, M.W. Witczak, R.F. Bonaquist, Asphalt mix master curve construction using sigmoidal fitting function with non-linear least squares optimization, Recent advances in materials characterization and modeling of pavement systems (2004) 83-101.
[39] H. Chen, D.M. Barbieri, X. Zhang, I. Hoff, Reliability of Calculation of Dynamic Modulus for Asphalt Mixtures Using Different Master Curve Models and Shift Factor Equations, Materials 15 (12) (2022) 4325.
[40] M.W. Witzcak, Simple performance test for superpave mix design, Transportation Research Board (2002).
[41] I.M. Asi, Laboratory comparison study for the use of stone matrix asphalt in hot weather climates, Constr. Build. Mater. 20 (10) (2006) 982–989.
[42] H.L. Von Quintus, J. Rauhut, T. Kennedy, Comparisons of asphalt concrete stiffness as measured by various testing techniques (with discussion), Association of Asphalt Paving Technologists Proceedings, (1982).